Available online at
https://jmeche.uitm.edu.my/browse-journals/regular-issue/regular-issue-2025-vol-22-3/

e-ISSN: 2550-164X

Journal of Mechanical Engineering 22(3) 2025, 38 – 49.

Journal of Mechanical Engineering

Optimization of Magnetorheological Elastomer Composition and Ferrous Particle Size for Enhanced Sound Absorption Performance

Ahmad Nabil Mohd Razali[1], Khisbullah Hudha[2], Zulkiffli Abd Kadir[1], Saiddi Ali Firdaus Mohamed Ishak[1*], Noor Amira Ilyanie Ruslan[1], Noor Hafizah Amer[1]

[1]*Department of Mechanical Engineering, Faculty of Engineering, Universiti Pertahanan Nasional Malaysia, Sungai Besi, Kuala Lumpur, Malaysia*
[2]*Faculty of Engineering and Architecture, Nizwa University of Oman*

ARTICLE INFO

Article history:
Received 26 March 2025
Revised 07 May 2025
Accepted 09 May 2025
Online first
Published 15 September 2025

Keywords:
Magnetorheological elastomers
sound absorption
Optimum composition

DOI:
https://doi.org/10.24191/jmeche.v22i3.5795

ABSTRACT

Nowadays, Magnetorheological Elastomers (MREs) are widely used in real applications such as vibration absorbers, isolators, magneto-resistors, and electromagnetic wave absorbers. The MR effect refers to the modulus feedback generated by MREs. When exposed to a magnetic field, the mechanical and viscoelastic properties of MREs can be reversibly altered. MREs are composite materials consisting of magnetizable particles embedded within a solid elastomer matrix. Their behavior is influenced by factors such as the type and size of the dispersed magnetic particles, the elastomer matrix composition, and the presence of non-magnetic fillers like plasticizers, carbon black, and crosslinking agents. This research investigates how the sound absorption capability of MREs is affected by their composition and the size of ferrous particles. The primary objective is to determine the optimal MRE composition for sound absorption and to analyze the impact of varying ferrous particle sizes on this property. MREs are synthesized using carbonyl iron particles, a hardener, and RTV silicone rubber. Since the performance of MREs actual applications is significantly influenced by the size of ferrous particles, experimental evaluations are conducted to determine the optimal parameters for MRE composition. Finally, the fabricated MREs are tested in a laboratory setting to assess their sound absorption capabilities. Based on the experimental tests, the optimal amounts of carbonyl iron particles, RTV silicone rubber, and hardener are 15 g, 9 g, and 0.45 g, respectively.

[1*] Corresponding author. *E-mail address*: saiddi@upnm.edu.my
https://doi.org/10.24191/jmeche.v22i3.5795

INTRODUCTION

The interaction between magnetic particles in magnetorheological (MR) materials gives rise to various phenomena such as magnetostriction, magneto-deformation and magneto-mechanical effects. There are several types of magnetorheological materials, classified based on their non-magnetic matrix, including MR fluid (MRF) (Harun et al., 2018; Li et al., 2024), MR elastomer (MRE) (Bastola et al., 2020; Hafeez et al., 2020; Hamid et al., 2023), MR foam (Rohim et al., 2022; Yang et al., 2022), MR grease (MRG) (Yang et al., 2024), MR polymer gel (MRPG) (Li et al., 2021; Maurya & Sarkar, 2022), and MR plastomer (MRP) (Li et al., 2025). Among all types of MR materials, MRF was the first to be developed and remains the most widely used due to its rapid change in rheological properties and ease of fabrication. The development of MRF began in the late 1980s. When exposed to a magnetic field, MRF undergoes a phase transition from a liquid to a semi-solid state. Common real applications of MRF include dampers, valves, and clutches (Choi et al., 2016). In 1983, Rigbi & Jilkén (1983) introduced MRE as a solid-state MR material. MREs typically have a rubber-like consistency, with ferrite particles embedded in the elastomer matrix to enhance their magnetic responsiveness. The ferrite particles serve to lock the internal structure of the matrix, improving the material's stability and mechanical properties. Additives such as silicone or surfactants may also be included to optimize performance. MREs exhibit tunable viscoelastic properties, making them useful for applications such as vibration absorbers, vibration isolators, and sandwich beam structures (Priyandoko et al., 2018; Sulatchaneenopdon et al., 2022; Syam & Muthalif, 2021).

In 2002, Wilson et al. (2002) introduced Magnetorheological Polymer Gel (MRPG), a type of MR elastomer in which magnetic particles are dispersed within a gel matrix. The primary purpose of MRPG was to enhance system stability by controlling initial viscosity and reducing particle sedimentation in the presence of a magnetic field. Later, Xu et al. (2011) introduced Magnetorheological Plastomer (MRP), where magnetic particles are embedded within a plasticine-like polymer matrix. MRP exhibited a stronger magnetorheological effect than traditional MREs due to its higher concentration of magnetic particles. Compared to MREs, MRFs are significantly softer and less versatile for structural applications (Dhiman et al., 2024). Over the past few decades, MREs have gained attention as an advanced material for vibration control and noise reduction technologies (Masa'id et al., 2023). Their mechanical properties and behavior are strongly influenced by the magnetic field, particularly the presence of carbonyl iron particles. Due to this tunability, MREs are being explored for innovative applications aimed at mitigating noise pollution. Devices such as vibration absorbers, vibration isolators, sensors, and adaptive beam structures have been developed utilizing MRE technology (Zhao et al., 2017; Bastola & Hossain, 2020; Samal et al., 2020). A vibration absorption system typically consists of two main units: a semi-active vibration absorption unit and a passive vibration isolation unit. These units are composed of key components, including a magnetic conductor, shearing sleeve, bobbin core, electromagnetic coil winding, and a circular cylinder MRE vulcanized between the shearing sleeve and bobbin core. The fundamental role of vibration absorbers is to dissipate and reduce vibration energy, thereby enhancing damping performance in mechanical systems. MRE absorbers, in particular, play a crucial role in damping elements, effectively minimizing unwanted vibrations and improving overall system stability (Choi & Wereley, 2022).

Vibration isolators are used to separate equipment or structures from sources of vibration, minimizing unwanted oscillations and improving stability. Generally, vibration isolators are classified into two main types: base isolation and force isolation. Additionally, they can be categorized as either active or passive devices. Magnetorheological elastomer (MRE) isolators offer several advantages, including reducing vibrations in heavy machinery and serving as variable stiffness devices (Dingxin et al., 2025). Furthermore, MREs can be utilized in the development of tuned mass dampers (TMDs), a highly effective strategy widely implemented in skyscrapers and bridges to mitigate structural dynamic responses. This is possible because the stiffness of MREs can be actively adjusted using an applied magnetic field (Wang et al., 2017). The MRE vibration isolator operates in both active and passive modes and consists of several key components, including a steel housing, non-magnetic bobbin, lower shaft, MRE mounts, and upper shaft. One significant

https://doi.org/10.24191/jmeche.v22i3.5795

advantage of this setup is its adaptability, as the vibration isolator can be positioned in different orientations depending on specific application requirements (Ubaidillah et al., 2018).

This research investigates the potential of MRE in noise absorption, exploring its capability to mitigate noise pollution by attenuating sound waves before they propagate into the environment. To maximize their effectiveness, optimizing the composition and size of ferrous particles within MREs is crucial. The primary challenge lies in identifying the optimal material composition, as different combinations significantly influence sound absorption performance. A higher concentration of ferromagnetic particles, particularly carbonyl iron particles, can enhance the internal structure of MREs when subjected to a magnetic field, thereby improving their acoustic absorption properties. In addition to composition, particle size plays a critical role in determining the density, magnetic responsiveness, and overall interaction of the particles within the elastomer matrix. Smaller particles tend to distribute more uniformly, enhancing compatibility with the elastomer, whereas larger particles may improve magnetic properties but potentially reduce the material's flexibility. Therefore, achieving an optimal particle size distribution is essential for balancing structural integrity, magnetic responsiveness, and acoustic performance to develop MREs with superior noise absorption capabilities.

EXPERIMENTAL SETUP FOR SOUND ABSORPTION TESTING

In order to fabricate the magnetorheological elastomer (MRE), several materials are required, namely carbonyl iron particles as the ferrous component, RTV silicone rubber as the rubber matrix, and a hardener. The carbonyl iron particles used have a size of 0.005 mm. Before pouring the mixture into the mold, a silicone spray is applied to the mold to prevent adhesion. Fig 1 shows the materials used for fabricating the MRE sample.

(a) (b) (c) (d)

Fig. 1. Material to fabricate MRE (a) carbonyl iron particle (b) hardener (c) silicon spray and (d) RTV silicon rubber.

The MRE is fabricated using a curing process at room temperature. Initially, a weighing scale is used to measure the materials as shown in Fig 2(a). The MRE mold shown in Fig 2(b) is used for the curing process. The first step involved scooping approximately 21 grams of carbonyl iron particles (size: 0.005 mm) and mixing them with 9 grams of RTV silicone rubber in an MRE mold. The mold is then sprayed with silicone spray to prevent the mixture from sticking to the mold walls, making it easier to remove the sample later. After that, 0.27 grams of hardening agent is added. The combined mixture is stirred uniformly until it changes to a greyish color, indicating that the carbonyl iron particles, RTV silicone rubber, and hardener are well combined. Once the mixture reached a semi-solid state, it was quickly poured into the mold as shown in Fig 2(c), to prevent premature hardening and to minimize air bubbles in the MRE sample. The curing process took one full day to ensure the MRE sample is completely cured, as illustrated in Fig

https://doi.org/10.24191/jmeche.v22i3.5795

2(d). After successfully completing the first stage of the MRE fabrication process, the next step is to fabricate MRE samples with different sizes of iron particles. The optimized material composition and corresponding applied currents are detailed in the authors' previous work (Sobri et al., 2024).

(a) (b) (c) (d)

Fig. 2. Process of making MRE sample (a) electronic balance (b) MRE mould (c) pre-hardening MRE sample and (d) MRE sample.

The size of the carbonyl iron particles (CIPs) is varied in the optimization process to develop a reliable MRE for sound absorption. The ferrous particle size plays a crucial role in determining the optimum composition and acoustic characteristics of the material. In this study, three different particle sizes namely 0.005 mm, 0.048 mm, and 0.052 mm are used as shown in Fig 3. These sizes range from extremely small to comparatively larger particles, allowing for a broader evaluation of their effects on sound absorption. The next step involves fabricating MRE samples using different CIP sizes while maintaining the optimum composition to maximize sound absorption capabilities.

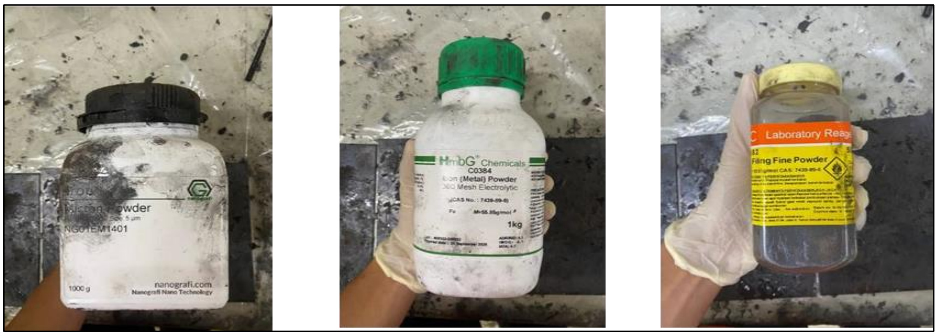

(a) (b) (c)

Fig. 3. Carbonyl iron particles (a) 0.005 mm, (b) 0.048 mm, and (c) 0.052 mm.

After successfully fabricating the MREs, experiments were conducted to evaluate their sound absorption capabilities (Gao & Zhang, 2021; Dogra & Gupta, 2024). Different material combinations were prepared in the laboratory, and tests were performed to analyze variations in sound absorption performance (Mahiou & Sadouki, 2024; Li et al., 2024). An impedance tube equipped with a sound level meter, a speaker, and an MRE sample was used in the experiment as shown in Fig 4(a). The MRE had a diameter of 5 cm and a thickness of 1 cm. Two sound level meters, designated as Sound Level Meter 1 and Sound Level Meter 2 were placed inside the impedance tube to measure sound absorption. The MRE was positioned between these two meters using a Teflon holder, as illustrated in Fig 4(b). To record

https://doi.org/10.24191/jmeche.v22i3.5795

measurements, both sound level meters were connected to a laptop. Additionally, the laptop was linked to a speaker, which was set to emit sound at a mid-frequency of 2000 Hz (Bradley, 2011) as shown in Fig 4(c). The sound levels recorded by both meters were analyzed and compared to assess the MRE's sound absorption performance.

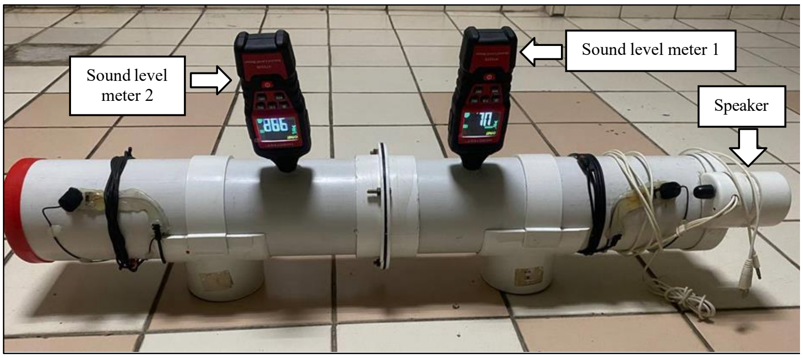

(a)

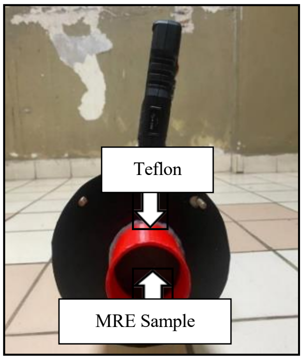

(b)

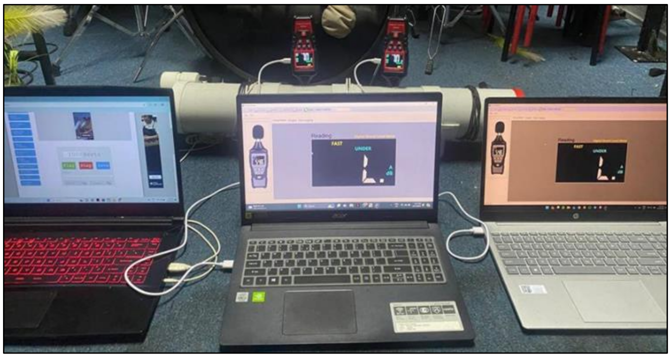

(c)

Fig. 4. Different material combinations in analyzing variations in sound absorption performance (a) impedance tube (b) setup MRE sample in the Teflon and (c) sound level meter and speaker are linked to the laptop.

EXPERIMENTAL RESULTS OF SOUND ABSORPTION USING MRE

This section discusses the findings from the experimental test of the MRE capabilities to absorb sound using an impedance tube. The optimum composition parameters are determined by calculating the signal-to-noise ratio (SNR). At the end of the section, the discussion of the influence of ferrous particle size on the sound absorption capabilities of MRE is discussed. The testing was done using a fabricated impedance tube and sound level meter, and the data was recorded. The experiment tested the sound absorption capability (SAC) using nine samples of MRE. Microphone 1 measured the maximum sound level from the speaker before it passed through the MREs, and Microphone 2 measured the maximum sound level after it passed through the MREs. The SAC of the MREs was recorded based on the difference in sound levels between Microphone 1 and Microphone 2. The SAC results are recorded in Table 1.

https://doi.org/10.24191/jmeche.v22i3.5795

Table 1. Experimental result

Sample	Microphone 1, dB	Microphone 2, dB	Sound Absorption capability, dB
1	96.43	66.43	30.00
2	98.53	69.03	29.50
3	101.80	79.63	22.17
4	100.30	79.53	20.77
5	95.10	64.47	30.63
6	95.20	62.13	33.07
7	97.00	80.30	16.70
8	98.80	81.57	17.23
9	100.40	80.10	20.30

In this experiment, each parameter is examined with nine samples. The frequency was fixed as 2000 Hz. The result of the nine experiments of SAC of MRE were totally different as the different reading values at microphone 1 and microphone 2. This was because the different composition of material is used to make the MRE sample. Sample 6 was chosen because of highest SAC of MRE compared to others sample. Fig 5 shows the sound absorption results of MRE.

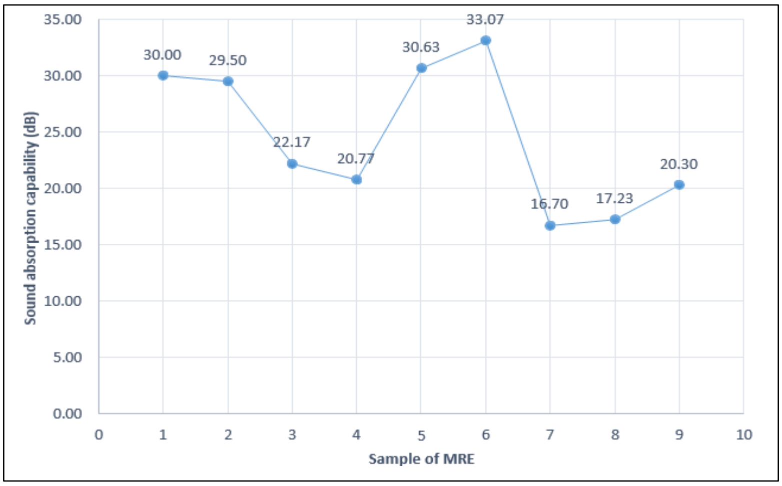

Fig. 5. Sound absorption capability of MRE.

SNR is the ratio between the strength of a signal and the strength of the background noise, showing effectiveness a sound absorption material works. A higher SNR means the signal is easier to detect. Table 2 shows the SNR results, which were calculated from the SAC values as shown in Equation 1.

$$SNR = -10log_{10}\left[\frac{1}{n}(\frac{SAC}{\sum SAC})^2\right] \tag{1}$$

Where:

SNR : Signal-to-Noise Ratio
SAC : Sound Absorption Capability
n : Total Number of Experiments

https://doi.org/10.24191/jmeche.v22i3.5795

Table 2. The calculation of Signal to Noise Ratio

Sample	Sound absorption capability, dB	Signal-to-noise ratio, dB
1	30.00	26.86
2	29.50	27.01
3	22.17	29.49
4	20.77	30.06
5	30.63	26.68
6	33.07	26.02
7	16.70	31.95
8	17.23	31.68
9	20.30	30.29

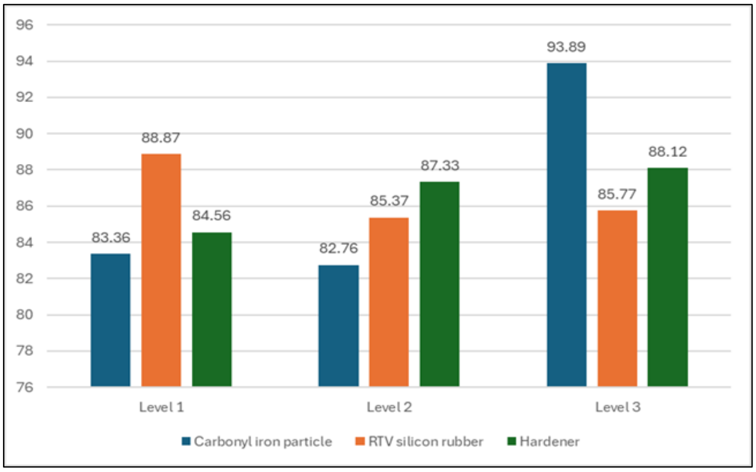

Fig. 6. The total of Signal to Noise ratio for different factors and levels.

Fig 6 represents the total SNR value for different factor and level. This graph aims to identify the optimum composition to maximize the sound absorption capability of MRE. The optimum composition was determined based on the highest SNR to obtain maximum SAC of MRE. In this study level 3, which is 15 g has been chosen for CIP to achieve optimum composition of MRE. This is because, higher concentration of CIP can improve the MRE density and stiffness but reduce their flexibility. A higher density might lead to less effective sound absorption when a material starts to reflect more than it absorbs. CIP are better distributed inside the elastomer matrix at lower concentrations. More homogeneous material with consistent acoustic characteristics can be produced by this uniform dispersion.

On the other hand, level 1 of RTV silicon rubber has the highest total SNR value for different factor and level compared to level 2 and level 3. RTV silicon rubber play a crucial role to provide elasticity and porosity to the MRE. To attain the ideal composition of MRE, level 1 or 9g of RTV silicon rubber has been selected for this project. This is because reducing RTV silicone rubber content can make the MRE more porous cause improving the way sound waves are absorbed and released. The contact between the carbonyl iron particles can be more apparent when there is less rubber, which helps to dissipate sound energy.

Other than that, level 3 of hardener has the highest total SNR value for different factor and level compared to level 1 and level 2. The hardener plays a critical role in the curing process and influencing the MRE's final mechanical properties. For this study, level 3 or 0.45g of hardener has been chosen to get the optimal composition of MRE. This can increase the microstructural stability of the MRE. This is because better dispersion and stabilization of the magnetic particles are made possible by a well-cured matrix which

https://doi.org/10.24191/jmeche.v22i3.5795

can enhance overall acoustic performance. Hereby, it could be said that 15 g of carbonyl iron particles, 9 g of RTV silicon rubber, and 0.45 g of hardener are the optimum composition as compared to other compositions. Various-sized ferrous particles can affect the sound absorption (Wu et al., 2020). Table 3 shows the SAC with different sizes of ferrous particles.

Table 3. Sound absorption with different sizes of ferrous particles

Size (mm)	Microphone 1, dB	Microphone 2, dB	Sound absorption capability, dB
0.005	95.2	62.13	33.07
0.048	97.7	71.60	26.10
0.052	96.6	71.50	25.10

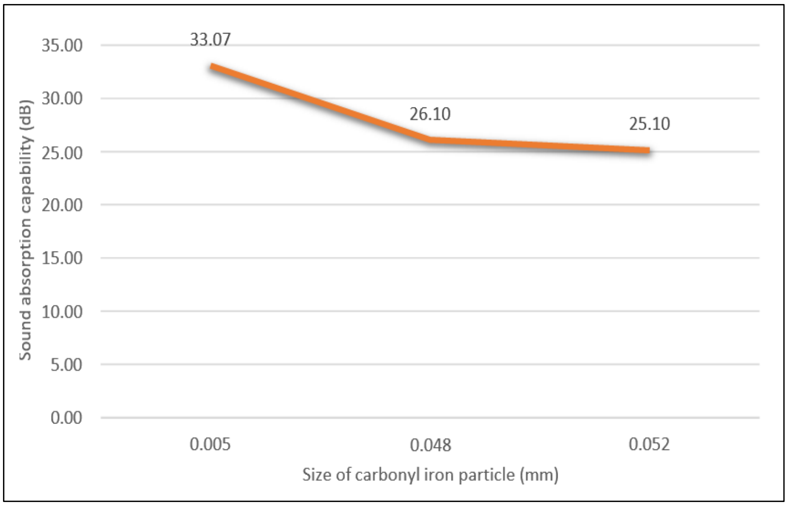

Fig. 7. Sound absorption capability of MRE for different size of CIP.

Fig 7 shows the sound absorption capacity of MRE samples with different carbonyl iron particle sizes. The lowest particle size, measuring 0.005 mm had the highest sound-absorbing ability at 33.07 dB. Sound absorption significantly decreases to 26.10 dB when the particle size rises to 0.048 mm. The absorption decreases again to 25.10 dB with a further increase to 0.052 mm indicating a small improvement in CIP size. This pattern suggests that smaller particle sizes are typically more effective in maximizing the sound absorption capability of MRE. The decrease in sound absorption with increasing particle size could be caused by a variety of factors. Smaller particles likely create a more uniform and densely packed structure inside the MRE, which could improve the material's ability to absorb sound waves. In contrast, larger particles could result in more spaces and flaws in the structure, decreasing the attenuation of sound waves (Wu et al., 2020).

From the overall experimental tests, the SAC for each composition and ferrous particle size was determined using the impedance tube test by comparing the readings from Microphone 1 and Microphone 2. The SNR was calculated using the SNR formula, and the optimal composition, as well as ferrous particle size, were identified based on the highest SNR values. The results showed that the optimal composition consisted of 15 g of carbonyl iron particles, 9 g of RTV silicone rubber, and 0.45 g of hardener. Additionally, the study analyzed the effect of different ferrous particle sizes and found that smaller particles yielded the highest SAC for MREs. SNR was used as a complementary metric to SAC for providing a more robust evaluation of the material's acoustic performance. While SAC quantifies how much sound energy is absorbed by the material at a given frequency, SNR helps assess the clarity or effectiveness of sound attenuation by comparing the absorbed signal to background noise. In this study, SNR was particularly

https://doi.org/10.24191/jmeche.v22i3.5795

useful for identifying the optimal MRE composition by highlighting the samples that not only absorbed sound effectively (high SAC) but also minimized unwanted noise transmission or reflection. Therefore, using SNR alongside SAC offers a more comprehensive analysis, ensuring that materials selected for noise control are both efficient absorbers in actual acoustic conditions.

CONCLUSION

Based on the experimental results and calculations in this study, there are several conclusions can be made. Firstly, the optimal composition and ferrous particle size for magnetorheological elastomers (MREs) to achieve maximum sound absorption capability (SAC) were identified. The best composition consisted of 15 g of carbonyl iron particles, 9 g of RTV silicone rubber, and 0.45 g of hardener. This combination yielded the highest signal-to-noise ratio (SNR) among the tested factors and levels, making it the most effective choice for enhancing the SAC of MREs. Secondly, the influence of ferrous particle size on the sound absorption capability of MREs was examined. The results indicated that ferrous particles with a size of 0.005 mm exhibited the highest sound absorption, making them the optimal particle size for maximizing the sound absorption coefficient (SAC) in MREs.

ACKNOWLEDGMENT

A high appreciation dedicated to Universiti Pertahanan Nasional Malaysia for the financial support and research facility for this research through “Geran Penyelidikan Jangka Pendek” numbered: (UPNM/2024/GPJP/TK/5).

CONFLICT OF INTEREST STATEMENT

All authors declare that they have no conflicts of interest.

AUTHORS’ CONTRIBUTIONS

The authors confirm their contribution to the paper as follows: **Fabrication of MRE and setup:** Ahmad Nabil Mohd Razali, Khisbullah Hudha, Saiddi Ali Firdaus Mohamed Ishak; **analysis of results and manuscript preparation**: Zulkiffli Abd Kadir, Noor Amira Ilyanie Ruslan, Noor Hafizah Amer; **calculation of SNR**: Ahmad Nabil Mohd Razali, Khisbullah Hudha, Zulkiffli Abd Kadir. All authors reviewed the results and approved the final version of the manuscript.

REFERENCES

Bradley, J. S. (2011). Review of objective room acoustics measures and future needs. Applied Acoustics, 72(10), 713-720.

Bastola, A. K., & Hossain, M. (2020). A review on magneto-mechanical characterizations of magnetorheological elastomers. Composites Part B: Engineering, 200, 108348.

https://doi.org/10.24191/jmeche.v22i3.5795

Bastola, A. K., Paudel, M., Li, L., & Li, W. (2020). Recent progress of magnetorheological elastomers: A review. Smart Materials and Structures, 29(12), 123002.

Choi, S. B., Li, W., Yu, M., Du, H., Fu, J., & Do, P. X. (2016). State of the art of control schemes for smart systems featuring magneto-rheological materials. Smart Materials and Structures, 25(4), 043001.

Choi, Y., & Wereley, N. M. (2022). Vibration isolation performance of an adaptive magnetorheological elastomer-based dynamic vibration absorber. Actuators, 11(6), 157.

Dhiman, N. K., Salodkar, S. M., Gagandeep, & Susheel, C. (2024). Advances in modeling and control of magnetorheological elastomers for engineering applications. Archives of Computational Methods in Engineering, 31(3), 1823–1865.

Dingxin, L., Xu, Z., Wenhao, F., Donghong, N., & Guijie, L. (2025). A tunable quasi-zero-stiffness vibration isolator (QZS-VI) with magnetorheological elastomer (MRE). Smart Materials and Structures, 34(3), 035026.

Dogra, S., & Gupta, A. (2024). Acoustic material testing using impedance tube. In Garg, N., Gautam, C., Rab, S., Wan, M., Agarwal, R., & Yadav, S. (Eds.), Handbook of Vibroacoustics, Noise and Harshness (pp. 1-13). Springer, Singapore.

Gao, N., & Zhang, Z. (2021). Optimization design and experimental verification of composite absorber with broadband and high efficiency sound absorption. Applied Acoustics, 183, 108288.

Hafeez, M. A., Usman, M., Umer, M. A., & Hanif, A. (2020). Recent progress in isotropic magnetorheological elastomers and their properties: A review. Polymers, 12(12), 3023.

Hamid, M. I. A., Mazlan, S. A., Nordin, N. A., Fatah, A. Y. A., Ubaidillah, Imaduddin, F., & Ismail, I. (2023). Design and dynamic stiffness evaluation of magnetorheological elastomer bushing using FEMM and dynamic testing machine. Journal of Mechanical Engineering, 20(1), 43-60.

Harun, M. H., Azhari, M. A., Yunos, R., Mat Yamin, A. K., & Sariman, M. Z. (2018). Characterization of a magnetorheological fluid damper applied to semi-active engine mounting system. Journal of Mechanical Engineering, 5(3), 248–259.

Li, L., Sun, Y., Gong, Y., Tong, Q., & Qi, L. (2024). Magnetorheological fluid for adaptive soft robotics. IEEE Robotics and Automation Letters, 10(1), 620-627.

Li, S., Li, Y., & Li, J. (2021). Thixotropy of magnetorheological gel composites: Experimental testing and modelling. Composites Science and Technology, 214, 108996.

Li, Y., Qi, S., Fu, J., Li, S., Liang, H., Zhu, P., Zhang, Y., & Yu, M. (2025). A hybrid magnetic-sensitive flexible structure with tunable energy absorption performance. Smart Materials and Structures, 34(3), 035049.

Li, Y., Dai, Y., Yao, G., Luo, W., Zhi, C., & Xing, Y. (2024). Design of an improved impedance tube to measure sound absorption coefficients of flexible textile materials. Engineering Research Express, 6(1), 015413.

Mahiou, A., & Sadouki, M. (2024). An inverse method based on impedance tubes for determining low-frequency non-acoustic parameters of rigid porous media. Journal of Vibration Engineering & Technologies, 12, 4119-4129.

Masa'id, A., Lenggana, B. W., Ubaidillah, U., Susilo, D. D., & Choi, S. B. (2023). A review on vibration control strategies using magnetorheological materials actuators: Application perspective. Actuators,

https://doi.org/10.24191/jmeche.v22i3.5795

12(3), 113.

Maurya, C. S., & Sarkar, C. (2022). Rheological and creep and recovery behavior of carbonyl iron water-based magnetorheological gel using laponite as an additive and oleic acid as a surfactant. Rheologica Acta, 61(2), 99–110.

Priyandoko, G., Kurniawan, T., & Soffie, S. M. (2018). Vibration control of magnetorheological elastomer beam sandwich. Proceeding of the Electrical Engineering Computer Science and Informatics (pp. 341-344). IEEE Publisher.

Rigbi, Z., & Jilkén, L. (1983). The response of an elastomer filled with soft ferrite to mechanical and magnetic influences. Journal of Magnetism and Magnetic Materials, 37(3), 267–276.

Rohim, M. A. S., Nazmi, N., Bahiuddin, I., Mazlan, S. A., Norhaniza, R., Yamamoto, S. I., Nordin, N. A., & Abdul Aziz, S. A. (2022). Prediction for magnetostriction magnetorheological foam using machine learning method. Journal of Applied Polymer Science, 139(34), e52798.

Sobri, N. S., Hudha, K., Kadir, Z. A., Amer, N. H., Ahmad, K. Z. K., & Rahmat, M. S. (2024). Parameter optimization of anisotropic polarization in magnetorheological elastomers for enhanced impact absorption capability using the Taguchi method. Journal of the Mechanical Behavior of Materials, 33(1), 20240003.

Samal, S., Škodová, M., Abate, L., & Blanco, I. (2020). Magneto-rheological elastomer composites. A review. Applied Sciences, 10(14), 4899.

Sulatchaneenopdon, N., Shen, Z., Son, H. W., Khantachawana, A., García-Barruetabeña, J., Elejabarrieta, M. J., Takahashi, T., Nakayama, T., & Niihara, K. (2022). Analyzing the influence of the core pre-structure on the dynamic response of a magnetorheological elastomer sandwich structure. Smart Materials and Structures, 31(7), 075027.

Syam, T. M. I., & Muthalif, A. G. A. (2021). Magnetorheological elastomer based torsional vibration isolator for application in a prototype drilling shaft. Journal of Low Frequency Noise, Vibration and Active Control, 41(2), 676-700.

Ubaidillah, Hadi, S., Harjana, Hairuddin, K., & Mazlan, S. A. (2018). Design and fabrication of magnetorheological elastomer vibration isolator. Journal of Mechanical Engineering, 5(6), 192–210.

Wang, Q., Dong, X., Li, L., & Ou, J. (2017). Study on an improved variable stiffness tuned mass damper based on conical magnetorheological elastomer isolators. Smart Materials and Structures, 26(10), 105028.

Wilson, M. J., Fuchs, A., & Gordaninejad, F. (2002). Development and characterization of magnetorheological polymer gels. Journal of Applied Polymer Science, 84(14), 2733–2742.

Wu, C., Cheng, C., El-Aty, A. A., Li, T., Qin, Y., Yang, Q., Hu, S., Xu, Y., & Guo, X. (2020). Influence of particles size and concentration of carbonyl iron powder on magnetorheological properties of silicone rubber-based magnetorheological elastomer. Materials Research Express, 7(8), 086101.

Xu, Y., Gong, X., Xuan, S., Zhang, W., & Fan, Y. (2011). A high-performance magnetorheological material: Preparation, characterization and magnetic-mechanic coupling properties. Soft Matter, 7(11), 5246–5254.

Yang, G., Pan, J., & Wang, D. (2024). A review on the magnetorheological materials and applications. International Journal of Applied Electromagnetics and Mechanics, 75(4), 407–443.

https://doi.org/10.24191/jmeche.v22i3.5795

Yang, J., Zhang, W., & Ge, X. (2022). Preparation and magneto-mechanical properties of 3D microporous magnetorheological foam. Journal of Intelligent Material Systems and Structures, 34(11), 1305–1313.

Zhao, L., Yu, M., Fu, J., Zhu, M., & Li, B. (2017). A miniature MRE isolator for lateral vibration suppression of bridge monitoring equipment: Design and verification. Smart Materials and Structures, 26(4), 047001.

https://doi.org/10.24191/jmeche.v22i3.5795